Microscopic Identification and Electronic Structure of a Di-Hydrogen–Vacancy Complex in Silicon by Optical Detection of Magnetic Resonance

W. M. Chen, O. O. Awadelkarim, and B. Monemar
Department of Physics and Measurement Technology, Linköping University, S-581 83 Linköping, Sweden

J. L. Lindström
Swedish Defense Research Establishment, Box 1165, S-581 11 Linköping, Sweden

G. S. Oehrlein
IBM Research Division, T. J. Watson Research Center, Yorktown Heights, New York 10598
(Received 7 August 1989; revised manuscript received 4 April 1990)

We present a microscopic identification of a hydrogen-related-complex defect in electron-irradiated, hydrogenated, boron-doped, single-crystalline silicon, by optical detection of magnetic resonance. The symmetry of this defect has been deduced as C_{2v}, and from the observed hyperfine interactions the defect is identified as a di-hydrogen–vacancy complex, where the H atoms passivate two of the four dangling bonds in a monovacancy. A spin triplet is the lowest electronic excited state of the defect, which exhibits a strong recombination channel for the free carriers.

PACS numbers: 61.70.Bv, 71.55.Ht, 76.70.Hb

Hydrogen in semiconductors has been a subject of numerous investigations in recent years, due to its fundamental as well as technological interest.[1] Atomic hydrogen can be inadvertently introduced into silicon during a number of common device processing and operation steps.[1] The ability of hydrogen in silicon to passivate the electrical properties of shallow acceptors, donors, and point defects is now well established.[1] This is derived from experimental results obtained by a variety of techniques and from extensive theoretical efforts. Recently, electron-spin resonance (ESR) was employed to study H-related defects in H-implanted Si.[2] In this Letter we report optically detected magnetic resonance (ODMR) for a hydrogen-vacancy-complex defect in silicon (denoted as HVH below). The results allow determination of both the geometrical and the electronic structure of the defect.

⟨100⟩ wafers of 10–20-Ω cm, boron-doped, Czochralski-grown, single-crystalline silicon were used in this work. Hydrogenation (or deuteration) was performed by exposing ≈8.0-cm-diam and 0.38-mm-thick wafers to an H_2 (or D_2) plasma. The procedure and conditions during the plasma treatment are described in Ref. 3. The samples cut from these wafers were then irradiated with 2.0-MeV monoenergetic electrons to a total fluence of $(0.5–1.0)\times10^{18}$ e^-/cm^2 at room temperature. The ODMR experimental setup used in this work is described elsewhere.[4]

The photoluminescence (PL) spectrum from such a sample at a low temperature is typically dominated by a number of broad bands.[3,5] We shall not discuss the origin of these PL bands, since as will be shown below they do not relate to the HVH-complex defect under study in this work. In Fig. 1 we show an ODMR spectrum of the HVH complex at 9.6 K via detection of these PL bands. This ODMR spectrum arises from a spin-triplet ($S=1$) state. Here the high-field ODMR lines around $g\approx2$ belong to the $\Delta M_S=\pm1$ microwave-induced electronic transitions, and the spectrum is complicated by many inequivalent sites of the same anisotropic HVH complex of low symmetry at this specific magnetic-field direction. The weak and nearly isotropic low-field ODMR lines are due to the formally forbidden $\Delta M_S=\pm2$ electronic transitions, which is a signature of ODMR from a spin triplet. The spin-triplet nature for the HVH complex is further consolidated by an observation of a level-anticrossing (LAC) effect for this defect, commonly observed for spin-triplet defects in semiconductors.

The spectral-dependence study of the ODMR signal

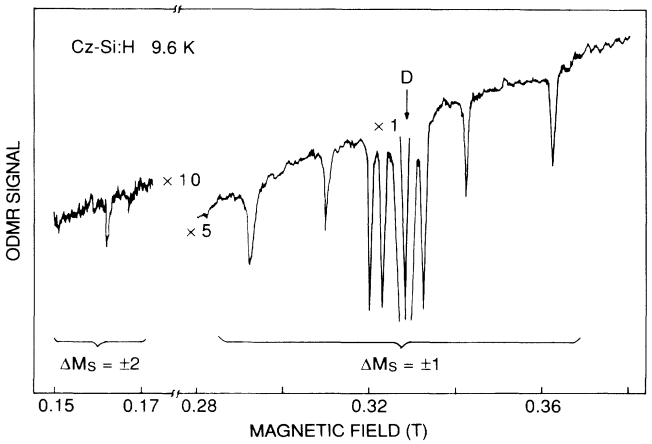

FIG. 1. ODMR spectrum of the HVH complex taken at 9.6 K and 9.16 GHz when **B** is close to the ⟨110⟩ direction, where both allowed $\Delta M_S=\pm1$ and formally forbidden $\Delta M_S=\pm2$ electronic transitions can be clearly seen. The central ODMR line, denoted as *D*, is not related to the HVH complex under study. The overall slope is induced by the heating effect of free carriers in the microwave field.

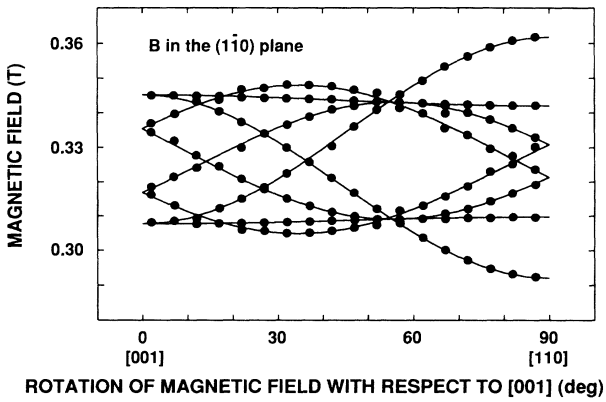

FIG. 2. Angular dependence of the ODMR spectra from the HVH complex. The dots represent the experimental results, and the lines are calculated by the spin Hamiltonian with the parameters given in Table I.

showed that the negative ODMR signal (Fig. 1) corresponds to a decrease in the entire range of PL emissions of various origins.[3,5] This strongly suggests that the HVH complex does *not* relate to any of these PL emissions. Further confirmation is provided by the results of a polarization study, where no polarization can be detected either in ODMR or in LAC. Instead, an indirect recombination process is involved,[6] linking the ODMR center (the HVH complex) and the PL centers. Among possible mechanisms, the competition in capture of free carriers is believed to be most efficient, since in this case no strong overlap of wave functions between the ODMR center and the PL centers is needed.[6]

The angular dependence of the ODMR spectrum has been obtained (Fig. 2) and analyzed with the aid of a spin Hamiltonian for a spin triplet,[7]

$$H_S=\mu_B\mathbf{B}\cdot\mathbf{g}\cdot\mathbf{S}+\mathbf{S}\cdot\mathbf{D}\cdot\mathbf{S}+\sum_j\mathbf{I}_j\cdot\mathbf{A}_j\cdot\mathbf{S}. \quad (1)$$

The terms in Eq. (1) describe the electronic Zeeman interaction, the fine-structure interaction, and the hyperfine (HF) interaction, respectively.[7] **S** ($S=1$) is the electronic spin of the excited state of the HVH complex where ODMR occurs. The evaluated spin-Hamiltonian parameters, obtained from the computer-generated fit to the experimental results (Fig. 2), are given in Table I.

A close look at the ODMR line shapes reveals a 1-2-1 HF intensity pattern when **B** is along one of the defect

TABLE I. Spin-Hamiltonian parameters for the HVH complex of C_{2v} symmetry studied in this work. **x**, **y**, and **z** denote the principal axes of the **g** and **D** tensors, as shown in Fig. 4.

Principal axes of the HVH complex	**g** tensor	**D** tensor (10^{-6} eV)
x≡[001]	2.002 ± 0.001	-1.44 ± 0.02
y≡[1$\bar{1}$0]	2.005 ± 0.001	-1.25 ± 0.02
z≡[110]	2.002 ± 0.001	2.69 ± 0.02

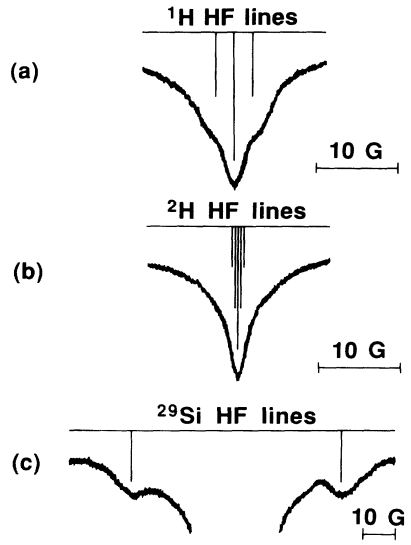

FIG. 3. The HF structure from (a) two ^{1}H atoms ($I=\frac{1}{2}$) and (b) two D (or ^{2}H) atoms ($I=1$) when **B**∥z. Stick diagrams are also shown as a guide for the eyes. (c) The HF structure from two equivalent ^{29}Si ligand atoms.

principal axes, as shown partly in Fig. 3(a) when **B**∥z. There are two alternative interpretations of this HF structure. It might arise from two equivalent nuclear spins with $I=\frac{1}{2}$. The only possible candidate for such species with appreciable concentration in the sample is then the ^{1}H atom ($I=\frac{1}{2}$ and 99.985% natural abundance). Alternatively, it could result from the ^{29}Si atom of $I=\frac{1}{2}$. Because of its small natural abundance (4.7%), the number of equivalent sites of such Si ligand atoms must be in the range 10–12 to account for the experimentally observed 1-2-1 HF structure pattern. HF structure from such a large number of ligand atoms, however, has generally been observed to be isotropic, in contrast to the anisotropic HF structure observed in this case (Table II). Based on this argument the first explanation seems to be the only plausible one. To further ascertain the involvement of the H atoms in the HVH

TABLE II. Hyperfine interaction and the LCAO coefficients α_j^2, β_j^2, and η_j^2 as deduced from the ^{1}H and ^{29}Si hyperfine structures. **x**, **y**, and **z** denote the principal axes of the **g** and **D** tensors, as shown in Fig. 4. The axially symmetric axis for the ^{29}Si HF tensor is along the [1$\bar{1}\bar{1}$] or [11$\bar{1}$] crystallographic axis.

Nucleus	No. of equivalent sites	**A** tensor (10^{-6} eV)	α_j^2	β_j^2	$\sum_j\eta_j^2$
^{1}H	2	$A_x^j=0.024\pm0.01$ $A_y^j=0.022\pm0.01$ $A_z^j=0.026\pm0.01$	1		0.009
^{29}Si	2	$A_\parallel^j=-0.910\pm0.01$ $A_\perp^j=-0.470\pm0.01$	0.10	0.90	0.68

defect, we have carried out ODMR studies on the D_2-plasma-treated samples. In these samples, we observed that the ODMR line shape is different from that seen in the H_2-plasma-treated samples (Fig. 3). The former do not show the 1-2-1 pattern. Instead a narrower ODMR line is generally observed as shown in Fig. 3(b), due to the smaller HF interaction (proportional to $g_N\mu_N$, where g_N is the nuclear g value and μ_N is the nuclear magneton) for the D atom (a factor of 6.5144 smaller than that of the H atom[8]). This evidence proves unambiguously the presence of the H atoms in the HVH defect complex.

Clearly the HVH complex studied here, containing two H atoms, could not be solely an H_2 molecule, since this is generally believed to be electrically and optically inactive in silicon.[1] The primary damage products after electron-irradiation include vacancies and self-interstitials (Si_I).[9] These native lattice defects, once produced by e^- irradiation, are unstable at room temperature. They are able to migrate throughout the sample during irradiation until trapped by impurities. To distinguish which type of the lattice defects is incorporated in the HVH complex, we have investigated the HF structure from the ^{29}Si atom, which is resolved in the ODMR spectra as shown in more detail in Fig. 3(c). The HF interactions are observed to contain two groups, and both are axially symmetric as listed in Table II, where one group has the symmetry axis closely along the $[\bar{1}\,\bar{1}\,\bar{1}]$ and the other along the $[11\bar{1}]$ crystallographic axis. The negative sign for the A-tensor components is due to the nuclear g value for the ^{29}Si nucleus being negative, i.e., $g_N(^{29}\mathrm{Si}) = -1.1106$. The intensity ratio of about $\sim 8\%$ between the ^{29}Si HF lines and the main ODMR peak (arising from the ^{28}Si and ^{30}Si of a total 95.3% natural abundance) indicates that there are two equivalent sites for such ^{29}Si atoms.

To get information on the degree of localization of the total wave function from the observed HF interactions, we have utilized a one-electron linear-combination-of-atomic-orbitals (LCAO) method.[10] In this method we assume that the wave function for the unpaired electron can be constructed as a LCAO centered on the atoms near the defect:

$$\Psi = \sum_j \eta_j \psi_j . \tag{2}$$

At each site j we approximate ψ_j as a hybrid ns-np orbital:

$$\psi_j = \alpha_j (\psi_{ns})_j + \beta_j (\psi_{np})_j , \tag{3}$$

where $n=3$ for Si. $\alpha_j^2+\beta_j^2=1$ and $\sum_j \eta_j^2 = 1$ as required by normalization neglecting overlap.[10] Assuming no contribution from the second-order perturbation, the axially symmetric A tensor from the jth ^{29}Si nucleus can be described as

$$A_{\parallel}^{j} = a_j + 2b_j , \tag{4}$$

$$A_{\perp}^{j} = a_j - b_j , \tag{5}$$

where

$$a_j = \tfrac{8}{3}\pi g_0 g_N \mu_B \mu_N \alpha_j^2 \eta_j^2 |\psi_{3s}(0)|_j^2 \tag{6}$$

and

$$b_j = \tfrac{2}{5} g_0 g_N \mu_B \mu_N \beta_j^2 \eta_j^2 \langle r_{3p}^{-3} \rangle_j . \tag{7}$$

g_0 is the electron g value, and μ_B is the Bohr magneton.

Using the values derived from the Hartree-Fock-Slater atomic orbitals, $|\psi_{3s}(0)|^2 = 34.52\times 10^{24}$ cm^{-3} and $\langle r_{3p}^{-3} \rangle = 18.16\times 10^{24}$ cm^{-3},[11] the parameters α_j^2, β_j^2, and η_j^2 are estimated and are given in Table II. It is concluded that about 68% of the wave function is localized at two equivalent Si ligand atoms. In addition, the hybrid orbital has a strong $3p$ character ($\sim 90\%$). This is a fingerprint of a vacancy-associated defect, possessing a very localized wave function.[12] A considerably delocalized wave function is, in contrast, typically observed for a Si_I-related defect.[13] Moreover, the g shift obtained for the HVH center falls into the category of vacancy-related defects.[14] It is suggested, therefore, from the HF structure, that a vacancy or a vacancy cluster participates in the HVH defect complexing. The even-number-vacancy defects can be excluded in this case, since they are not consistent with the symmetry and anisotropy deduced for the **g** and **A** tensors.[12] To determine whether a one-vacancy or an odd-number- (more than one) vacancy defect is involved, we have attempted to estimate the principal values of the **D** tensor assuming a magnetic dipole-dipole (d-d) interaction. These values ($\sim 10^{-6}$ eV) are only consistent with that for a one-vacancy defect. The D-tensor values for multivacancy defects are at least 1 order of magnitude lower, since the magnetic d-d interaction decreases drastically as $\sim r^{-3}$ with increasing separation r between the dipoles.[7] We conclude that the only appropriate model for the HVH defect identity is a di-hydrogen–vacancy complex (Fig. 4), in full agreement with the C_{2v} symmetry obtained for this HVH complex from the angular dependence study of the ODMR spectrum (Fig. 2).

With the aid of the LCAO method and the value $|\psi_{1s}(0)|^2 = 2.148\times 10^{24}$ cm^{-3} for the free hydrogen atom,[15] we estimate that only about 0.9% of the wave function of the unpaired electrons is localized at the two H atoms. This is not at all surprising since the H atoms passivate efficiently two of the four broken bonds near the vacancy, so that the wave function of the unpaired electrons are highly localized on the molecular orbital formed between the other two unpassivated dangling bonds (Fig. 4). This is consistent with the observed strong localization ($\sim 68\%$) of the wave function at the two Si atoms bridged by the molecular orbital. Previous ESR on Si-H centers in Si also reached a similar conclusion that the interaction between the unpaired electron and the H nucleus is indeed weak.[2]

The electronic structure of the HVH complex can be discussed in terms of a two-electron model, schematically

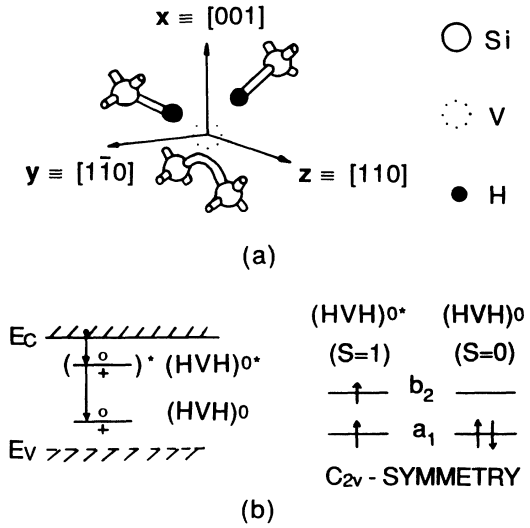

FIG. 4. Schematic results for the HVH complex: (a) the model for the defect identity, and (b) the electronic structure, including the energy levels in the band gap and the recombination processes involved. In (b) only the capture of the free electrons is shown. A similar picture can be obtained for the processes involving the capture of the free holes. See text for a more detailed discussion.

shown in Fig. 4. Parallel spins of the two spinlike ($S=\frac{1}{2}$) electrons lead to a paramagnetic spin triplet as the lowest electronic excited state of the neutral HVH complex. The ground state may naturally be expected to be diamagnetic ($S=0$), when spins pair off. The recombination process upon optical excitation can be understood as follows. First, a photoexcited free electron (or hole) is captured by the $(HVH)^+$ [or $(HVH)^-$] complex forming an excited state $(HVH)^{0*}$ of the neutral HVH center, where one electron is lying in the the excited antibonding state b_2 and the other electron remains in the bonding state a_1. Parallel spins of these two bound electrons give rise to a spin triplet. The HVH center subsequently makes a transition from the excited state $(HVH)^{0*}$ to its singlet ground state $(HVH)^0$; i.e., the excited electron makes a transition from the b_2 state to the a_1 state where the two spins are paired off.

To summarize, we list the main results from this work: (i) The HVH center has been created during e^- irradiation, with dangling bonds partially passivated, and acts as a strong recombination channel for the free carriers; (ii) the defect has been identified as a di-hydrogen–vacancy (HVH) complex, consistent with all experimental results; (iii) a spin triplet is identified to be the lowest electronic excited state of the HVH complex in its neutral charge state where the ODMR occurs; (iv) the prevalence of defect interaction involving hydrogen (i.e., hydrogen complexing with other defects) and the ability of hydrogen to passivate the electrical activity of dangling bonds have been demonstrated. This work provides, to the best of our knowledge, the first ODMR study on the electronic structure and the microscopic identification of a hydrogen-related-complex defect in a semiconductor. The important experimental background to this work is that indirect recombination processes enable us to apply the ODMR technique even to strongly nonradiative defects in silicon.

We are grateful to J. H. Svensson, J. Weber, and J. W. Corbett for valuable discussions.

[1]For a recent review, see, e.g., S. J. Pearton, J. W. Corbett, and T. S. Shi, Appl. Phys. A **43**, 153 (1987), and references therein.

[2]Yu. V. Gorelkinskii and N. N. Nevinnyi, Pis'ma Zh. Tekh. Fiz. **13**, 105 (1987) [Sov. Tech. Phys. Lett. **13**, 45 (1987)].

[3]H. Weman, J. L. Lindström, G. S. Oehrlein, and B. G. Svensson, J. Appl. Phys. **67**, 1013 (1990).

[4]W. M. Chen and B. Monemar, Phys. Rev. B **40**, 1365 (1989).

[5]M. Singh, J. Weber, T. Zundel, M. Konuma, and H. Cerva, Mater. Sci. Forum **38–41**, 1033 (1989).

[6]W. M. Chen, O. O. Awadelkarim, H. Weman, and B. Monemar, Phys. Rev. B **40**, 10013 (1989).

[7]A. Abragam and B. Bleaney, *Electronic Paramagnetic Resonance of Transition Ions* (Clarendon, Oxford, 1970).

[8]*CRC Handbook of Chemistry and Physics* (CRC Press, Boca Raton, FL, 1989).

[9]G. D Watkins, in *Deep Centers in Semiconductors,* edited by S. T. Pantelides (Gordon and Breach, New York, 1986), p. 147.

[10]G. D. Watkins and J. W. Corbett, Phys. Rev. **121**, 1001 (1961).

[11]J. R. Morton and K. F. Preston, J. Mag. Reson. **30**, 577 (1978).

[12]Y.-H. Lee and J. W. Corbett, Phys. Rev. B **13**, 2653 (1976).

[13]Y.-H. Lee, N. N. Gerasimenko, and J. W. Corbett, Phys. Rev. B **14**, 4506 (1976).

[14]E. G. Sieverts, Phys. Status Solidi (b) **120**, 11 (1983).

[15]A. Carrington and A. D. McLachlan, *Introduction to Magnetic Resonance* (Harper & Row, New York, 1967).